Supplemental material to this article can be found at:
http://dmd.aspetjournals.org/content/suppl/2010/07/30/dmd.110.034348.DC1.html

0090-9556/10/3811-2032–2039$20.00
DRUG METABOLISM AND DISPOSITION
Vol. 38, No. 11
34348/3631113
DMD 38:2032–2039, 2010
Printed in U.S.A.
Copyright © 2010 by The American Society for Pharmacology and Experimental Therapeutics

Drug Metabolism and Pharmacokinetics of 4-Substituted Methoxybenzoyl-aryl-thiazoles[S]

Chien-Ming Li, Yan Lu, Ramesh Narayanan, Duane D. Miller, and James T. Dalton

GTx Inc., Memphis, Tennessee (C.-M.L., R.N., D.D.M., J.T.D.); Division of Pharmaceutics, College of Pharmacy, The Ohio State University, Columbus, Ohio (C.-M.L., J.T.D.); and Department of Pharmaceutical Sciences, University of Tennessee Health Science Center, Memphis, Tennessee (Y.L., D.D.M.)

Received May 7, 2010; accepted July 30, 2010

ABSTRACT:

Tubulins are some of the oldest and most extensively studied therapeutic targets for cancer. Although many tubulin polymerizing and depolymerizing agents are known, the search for improved agents continues. We screened a class of tubulins targeting small molecules and identified 4-(3,4,5-trimethoxybenzoyl)-2-phenyl-thiazole (SMART-H) as our lead compound. SMART-H inhibited the proliferation of a variety of cancer cells in vitro, at subnanomolar IC_{50}, and in vivo, in nude mice xenografts, with near 100% tumor growth inhibition. Metabolic stability studies with SMART-H in liver microsomes of four species (mouse, rat, dog, and human) revealed half-lives between <5 and 30 min, demonstrating an interspecies variability. The clearance predicted based on in vitro data correlated well with in vivo clearance obtained from mouse, rat, and dog in vivo pharmacokinetic studies. SMART-H underwent four major metabolic processes, including ketone reduction, demethylation, combination of ketone reduction and demethylation, and hydroxylation in human liver microsomes. Metabolite identification studies revealed that the ketone and the methoxy groups of SMART-H were most labile and that ketone reduction was the dominant metabolism reaction in human liver microsomes. We designed and tested four derivatives of SMART-H to improve the metabolic stability. The oxime and hydrazide derivatives, replacing the ketone site, demonstrated a 2- to 3-fold improved half-life in human liver microsomes, indicating that our prediction regarding metabolic stability of SMART-H can be extended by blocking ketone reduction. These studies led us to the next generation of SMART compounds with greater metabolic stability and higher pharmacologic potency.

Introduction

Cancer is the second leading cause of death in the United States, with 500,000 people estimated to die from the disease in 2010 (Cancer Facts and Figures 2010, American Cancer Society Website, http://www.cancer.org). Despite multiple pathways being used for the development of novel therapeutic agents, tubulins remain an attractive target to treat cancer (Carlson, 2008; Zhao et al., 2009). However, most of the tubulin polymerizing and depolymerizing agents are P-glycoprotein substrates, leading to the development of resistance over a prolonged period of treatment (Perez, 2009).

Recently our group developed a series of 4-substituted methoxybenzoyl-aryl-thiazole (SMART) compounds that bind to the colchicine-binding site and inhibit tubulin polymerization and cancer cell growth at low nanomolar concentrations (Lu et al., 2009). In addition, the SMART compounds were not substrates of P-glycoprotein and retained potent anticancer activity demonstrated both in vitro and in vivo in wild-type and resistant cancer cells (C. M. Li, Z. Wang, Y. Lu, W. Li, S. Ahn, R. Narayanan, J. D. Kearbey, D. N. Parke, D. D. Miller, and J. T. Dalton, manuscript submitted for publication).

Pharmacokinetics and metabolism play important roles in lead optimization as they affect the exposure and thus efficacy of drugs (Pelkonen et al., 2005). Many molecules that were demonstrated to be potent in vitro failed in vivo because of poor pharmacokinetic (PK) properties. A potential drug candidate is expected to be cleared slowly from the system and to have sufficient exposure to elicit its action. Identification of chemical or functional groups or so-called "soft spots" is a key first step in the design of compounds with better metabolic stability (Zhang et al., 2007). Liver microsomes, which contain several key enzymes such as cytochrome P450s, flavin monooxygenases, and glucuronosyltransferases, all required for drug metabolism, are widely used for in vitro metabolic stability studies. In vitro microsomal stability assays not only facilitate the selection of compounds with greater metabolic stability but are also useful to identify metabolites of the parent molecule (Huang and Ho, 2009).

In this study, we identified the metabolites and PK properties of one of the SMART compounds, SMART-H, using in vitro liver microsomes and PK studies. We also identified the labile sites and devel-

Article, publication date, and citation information can be found at http://dmd.aspetjournals.org.
doi:10.1124/dmd.110.034348.
[S] The online version of this article (available at http://dmd.aspetjournals.org) contains supplemental material.

ABBREVIATIONS: SMART, 4-substituted methoxybenzoyl-aryl-thiazole; SMART-H, 4-(3,4,5-trimethoxybenzoyl)-2-phenyl-thiazole; DMSO, dimethyl sulfoxide; LC, liquid chromatography; MS/MS, tandem mass spectrometry; THF, tetrahydrofuran; MS, mass spectrometry; ESI, electrospray ionization; SMART-213, pentafluorophenyl-(2-phenyl-thiazol-4-yl)-methanone; SMART-176A, [(2-phenyl-thiazol-4-yl)-(3,4,5-trimethoxyphenyl)-methylene]-hydrazine; SMART-173A, (2-phenylthiazol-4-yl)(3,4,5-trimethoxyphenyl)methanone oxime; SMART-329, 2-phenyl-4-(3,4,5-trimethoxyphenyl)thiazole.

Downloaded from dmd.aspetjournals.org at ASPET Journals on March 18, 2015

oped the next generation of SMART compounds having better metabolic stability with little or no impact on potency.

Materials and Methods

Metabolic Stability Studies. Incubations for metabolic stability studies were conducted in a 1-ml reaction volume containing 0.5 μM (final concentration) SMART-H or other test compounds and 1 mg/ml microsomal protein (mouse, rat, dog, and human liver microsomes; XenoTech, LLC, Kansas City, MO) in reaction buffer [0.2 M phosphate buffer solution (pH 7.4), 1.3 mM $NADP^+$, 3.3 mM glucose 6-phosphate, and 0.4 U/ml glucose-6-phosphate dehydrogenase] at 37°C in a shaking water bath. SMART-H, at 50 μM concentration, with the above-mentioned conditions, was used for metabolite identification studies. For glucuronidation studies, 2 mM UDP-glucuronic acid (Sigma-Aldrich, St. Louis, MO) cofactor in deionized water was incubated with 8 mM $MgCl_2$, 25 μg of alamethicin (Sigma-Aldrich) in deionized water, and NADPH-regenerating solutions (BD Biosciences, San Jose, CA) as described previously. The total DMSO concentration in the reaction solution was approximately 0.5% (v/v). Aliquots (100 μl) from the reaction mixtures were sampled at 5, 10, 20, 30, 60, and 120 min, and acetonitrile (150 μl) containing 100 nM internal standard (an analog of SMART-H) was added to quench the reaction and to precipitate the proteins. Samples were then centrifuged at 4000*g* for 15 min at room temperature, and the supernatant was analyzed directly by LC-MS/MS.

Protein Binding Assay. Plasma protein binding studies of SMART-H were conducted by the ultrafiltration technique. One milliliter of mouse, rat, dog, and human plasma (Thermo Fisher Scientific, Waltham, MA) samples was spiked with 5 μl of 100 μM SMART-H and incubated at 37°C for 30 min before ultrafiltration. Samples (400 μl) were transferred to Amicon centrifugal filter devices (30-kDa molecular mass cutoff; Millipore Corporation, Billerica, MA) and centrifuged at 14,000*g* for 20 min. An aliquot (50 μl) of the ultrafiltrate was combined with 150 μl of acetonitrile containing an internal standard for LC-MS/MS analysis. Protein binding of SMART-H in mouse, rat, dog, and human microsomes was performed using 0.5 μM SMART-H and 1 mg/ml microsomal proteins in the absence of NADPH. The incubation conditions and sample preparation were the same as those described for plasma protein binding.

Prediction of In Vivo Clearance of SMART-H in Mouse, Rat, Dog, and Human. In vivo clearance was predicted using the data obtained from metabolic stability (half-life in liver microsomes) and protein binding in plasma and liver microsomes studies. The intrinsic hepatic clearance ($Cl_{i,\ in\ vitro}$) of SMART-H was determined using the equation: $Cl_{i,\ in\ vitro} = [0.693/(t_{1/2}$ in minutes · protein concentration in milligrams per milliliter)]. The intrinsic clearance was then scaled to predict clearance that would occur in the liver in vivo. Scaling factors (milligrams of protein per gram of liver · gram of liver per kilogram body weight) are 2400, 1815, and 1980 for rat, dog, and human, respectively (Baarnhielm et al., 1986; Smith et al., 2008). In vivo intrinsic hepatic clearance ($Cl_{i,\ h}$, milliliters per minute per kilogram body weight) in liver was estimated by multiplying $Cl_{i,\ in\ vitro}$ by the scaling factors. In vivo hepatic clearance (Cl_h) was estimated by incorporating estimates of $Cl_{i,\ h}$, Q_h, and f_u into the well stirred model (venous equation): $Cl_h = [Q_h \cdot f_{u,\ p} \cdot (Cl_{i,\ h}/f_{u,\ m})]/[Q_h + f_{u,\ p} \cdot (Cl_{i,\ h}/ f_{u,\ m})]$ (Chiba et al., 2009). Q_h, $f_{u,\ p}$, and $f_{u,\ m}$ represent hepatic blood flow, fraction unbound in plasma, and fraction unbound in microsomes, respectively.

Pharmacokinetic Studies. All animal studies were conducted under the auspices of a protocol reviewed and approved by the Institutional Laboratory Animal Care and Use Committee of The University of Tennessee. SMART-H (15 mg/kg) was dissolved in PEG300-DMSO (1:4) and administered once intravenously into the tail vein of 6- to 8-week-old ICR mice ($n = 3$ per each time point; Harlan Inc., Indianapolis, IN). Blood samples were collected in heparinized tubes via cardiac puncture under isoflurane anesthesia at 2, 5, 15, and 30 min and 1, 2, 4, 8, 16, and 24 h after administration. Plasma samples were collected by centrifugation at 8000*g* for 5 min and stored immediately at −80°C for further analysis.

SMART-H was administered intravenously into the thoracic jugular vein (catheters from Braintree Scientific Inc., Braintree, MA) of male Sprague-Dawley rats ($n = 4$; 254 ± 4 g; Harlan, Indianapolis, IN) at 2.5 mg/kg (in PEG300-DMSO, 1:4). An equal volume of heparinized saline was injected to replace the removed blood, and blood samples (250 μl) were collected via the jugular vein catheters at 10, 20, and 30 min and 1, 2, 4, 8, 12, 24, and 48 h. All syringes and vials were heparinized for blood collection. Plasma samples were obtained as described previously.

A female beagle dog weighing 11.2 kg was used in this study. The animal was fasted overnight and until 2 h after drug administration. The dog was given a single intravenous dose of SMART-H (0.25 mg/kg, in PEG300-DMSO, 1:4). Blood was drawn at 10, 20, and 30 min and 1, 2, 4, 8, 12, 24, 48, and 96 h. Plasma samples were obtained as described previously.

SMART-H was extracted from 100 μl of plasma with 200 μl of acetonitrile containing 100 nM internal standard. The samples were thoroughly mixed and centrifuged, and the organic extract was transferred to an autosampler for LC-MS/MS analysis. The PK parameters were determined using noncompartmental analysis (WinNonlin; Pharsight, Mountain View, CA).

Analytical Method. Sample solution (10 μl) was injected into an high-performance liquid chromatography system (Agilent 1100 Series Chemstation; Agilent Technologies, Santa Clara, CA). SMART-H and its metabolites were separated on a narrow-bore C4 column (2.1 × 150 mm, 5 μm; Varian Inc., Palo Alto, CA). Two gradient modes were used. For metabolic stability, the gradient mode was used to achieve the separation of analytes using mixtures of mobile phase A [acetonitrile-H_2O (5:95%) containing 0.1% formic acid] and mobile phase B (acetonitrile-H_2O (95:5%) containing 0.1% formic acid) at a flow rate of 300 μl/min. Mobile phase A was used at 55% from 0 to 0.5 min followed by a linearly programmed gradient to 100% of mobile phase B within 2.5 min; 100% of mobile phase B was maintained for 1 min before a quick ramp up to 55% mobile phase A. Mobile phase A was continued for another 8 min toward the end of analysis. For metabolite identification studies, a slower gradient mode was used to achieve the separation of analytes with the same flow rate and mobile phase A and B as described. Mobile phase A was used at 20% from 0 to 1 min followed by a linearly programmed gradient to 100% of mobile phase B within 17 min; 100% of mobile phase B was maintained for 2 min before a quick ramp up to 20% mobile phase A. Mobile phase A was continued for another 25 min toward the end of analysis.

A triple-quadruple mass spectrometer (API Qtrap 4000; Applied Biosystems/MDS SCIEX, Concord, ON, Canada) operating with a TurboIonSpray source was used. The spraying needle voltage was set at 5 kV for positive mode. Curtain gas was set at 10; gas 1 and gas 2 were set at 50, collision-assisted dissociation gas at medium, and the source heater probe temperature at 500°C. Data acquisition and quantitative processing were accomplished using Analyst software (version 1.4.1; Applied Biosystems).

Cell Culture and Cytotoxicity Assay of Prostate Cancer. We examined the antiproliferative activity of the SMART compounds in four human prostate cancer cell lines, LNCaP, DU 145, PC-3, and PPC-1 (American Type Culture Collection, Manassas, VA). Cells were cultured in RPMI 1640 (Mediatech, Inc., Manassas, VA) supplemented with 10% fetal bovine serum (Mediatech) and were maintained at 37°C in a humidified atmosphere containing 5% CO_2. Depending on cell types, 1000 to 5000 cells were plated into each well of 96-well plates and exposed to different concentrations of the compound of interest for 96 h. At the end of the treatments, cell viability was measured using the sulforhodamine B assay. Percentage of cell survival was plotted against drug concentrations and the IC_{50} values (concentration that inhibited cell growth by 50% of untreated control) were obtained by nonlinear regression analysis using WinNonlin.

Synthesis of SMART Compounds. All reagents were purchased from Sigma-Aldrich, Fisher Scientific, AK Scientific (Mountain View, CA), and Oakwood Products (West Columbia, SC) and were used without further purification. Moisture-sensitive reactions were performed under an argon atmosphere. Routine thin-layer chromatography was performed on aluminum-backed Uniplates (Analtech, Newark, DE). NMR spectra were obtained on an Bruker AX 300 (Bruker, Newark, DE) spectrometer or an Inova 500 spectrometer (Varian, Inc., Palo Alto, CA). Chemical shifts are reported as parts per million relative to tetramethylsilane in $CDCl_3$. Mass spectral data were collected on a Bruker ESQUIRE electrospray/ion trap instrument in positive and negative ion modes.

Synthesis of Putative Metabolites (Reduction of the Carbonyl Group in SMART-H). *Synthesis of (2-phenyl-thiazol-4-yl)-(3,4,5-trimethoxyphenyl)-methanol.* SMART-H (355 mg, 1 mmol) was dissolved in anhydrous THF and cooled to −78°C. Lithium aluminum hydride (1 M solution in THF; 1 ml) was added dropwise under argon protection. After completion of the reaction,

Downloaded from dmd.aspetjournals.org at ASPET Journals on March 18, 2015

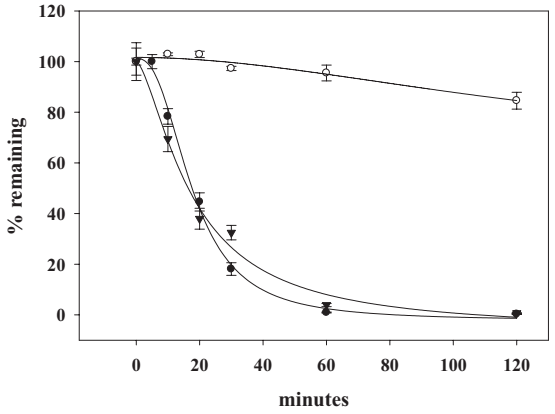

FIG. 1. Phase I metabolic stability of SMART-H in human liver microsome in the presence of NADPH (●) and in the absence of NADPH (○). ▼, phase I + II metabolic stability in the presence of NADPH and UDP-glucuronic acid. Values represent the mean ± S.D. of triplicate experiments.

excess lithium aluminum hydride was destroyed with ethyl acetate and then quenched with 20% H_2SO_4 solution. The organic layer was washed with brine, dried over anhydrous $MgSO_4$, filtered, and evaporated under reduced pressure. The residue was purified by column chromatography to give the compound as light yellow crystals (252 mg; 71% yield). ^{1}H NMR (300 MHz, $CDCl_3$): δ 7.96–7.93 (q, 2H), 7.44–7.42 (m, 3H), 6.97 (s, 1H), 6.76 (s, 2H), 5.93 (d, 1H), 3.86 (s, 9H). MS (ESI) *m/z* 380.1 $[M + Na]^+$, 355.9 $[M - H]^-$.

SMART-213: synthesis of pentafluorophenyl-(2-phenyl-thiazol-4-yl)-methanone. To a solution of pentafluorophenylmagnesium bromide (0.5 M, 2.7 ml) in 2 ml of THF was charged a solution of 2-phenyl-4, 5-dihydrothiazole-4-carboxylic acid methoxymethylamide (227 mg, 0.915 mmol) in 3 ml of THF at 0°C. The mixtures were stirred for 30 min until amides disappeared on thin-layer chromatography plates. The reaction mixture was quenched with saturated NH_4Cl, extracted with ethyl ether, and dried with $MgSO_4$. The solvent was removed under reduced pressure to yield a crude product, which was purified by column chromatography to obtain pure compound SMART-213 (147 mg) as a yellow solid. Yield: 45.2%. ^{1}H NMR (300 MHz, $CDCl_3$): δ 8.30 (s, 1H), 7.82–7.80 (m, 2H), 7.40–7.37 (m, 3H). ^{13}C NMR (75.5 MHz, $CDCl_3$): δ 178.7, 169.0, 154.3, 146.3, 144.8, 142.6, 140.2, 132.5, 131.1, 129.1, 128.3, 126.9. ^{19}F NMR (282.4 MHz, $CDCl_3$): δ −33.81, −44.89, −44.96. MS (ESI) *m/z* 378.0 $[M + Na]^+$.

SMART-176A: synthesis of [(2-phenyl-thiazol-4-yl)-(3,4,5-trimethoxyphenyl)-methylene]-hydrazine. A solution of SMART-H (230 mg, 0.65 mmol) in 2 ml of CH_2Cl_2 was added to a hot solution of hydrazine in 3 ml of ethanol and refluxed overnight. After completion of the reaction, the residue was absorbed on silica gel and purified by column chromatography to give compound SMART-176A as a mixture of isomers (136 mg; 57% yield). ^{1}H NMR (500 MHz, $CDCl_3$): δ 8.01–7.99 (m, 2H), 7.50–7.48 (m, 3H), 7.46 (br, 2H), 7.34 (s, 1H), 6.82 (s, 2H), 5.93 (d, 1H), 3.87 (s, 3H), 3.85 (s, 6H). MS (ESI) *m/z* 370.1 $[M + H]^+$.

SMART-173A: synthesis of (2-phenylthiazol-4-yl)(3,4,5-trimethoxyphenyl)methanone oxime. To a suspension of SMART-H (50 mg, 0.14 mmol) in 2 ml of ethanol was added an aqueous solution (0.5 ml) of hydroxylamine hydrochloride (34 mg, 0.49 mmol). Then 0.5 ml of 1 N NaOH was added dropwise to the reaction mixture, and the mixture was stirred at 55°C for 3 h. After completion of the reaction, the residue was absorbed on silica gel and purified by column chromatography to give compound SMART-173A (26 mg; 50% yield). ^{1}H NMR (300 MHz, DMSO-d_6): δ 11.95 (s, 1H), 8.35, 8.34 (s, s, 1H), 7.91–7.89 (m, 2H), 7.50–7.44 (br, 3H), 7.34 (s, 1H), 6.85, 6.85 (s, s, 1H), 5.93 (d, 1H), 3.73, 3.73 (s, s, 6H), 3.71, 3.70 (s, s, 3H). MS (ESI) *m/z* 393.1 $[M + Na]^+$, 368.9 $[M - H]^-$.

SMART-329: synthesis of 2-phenyl-4-(3,4,5-trimethoxyphenyl)thiazole. 2-Bromo-1-(3,4,5-trimethoxyphenyl)ethanone was prepared as reported previously (Sun et al., 2004). To a 10-ml round-bottom flask with a magnetic stir bar was added 2-bromo-1-(3,4,5-trimethoxyphenyl)ethanone (0.5 mmol) and ethanol (2.5 ml). Benzothioamide (0.5 mmol) was then added, and the mixture was refluxed for 1 h. After completion of the reaction, the residue was absorbed on silica gel and purified by flash chromatography on silica gel to give SMART-329 (167 mg; 51% yield). ^{1}H NMR (300 MHz, DMSO-d_6): δ 8.05–8.03 (m, 2H), 7.48–7.44 (m, 3H), 7.41 (s, 1H), 7.22 (s, 2H), 3.97 (s, 6H), 3.89 (s, 3H). MS (ESI) *m/z* 350.1 $[M + Na]^+$.

Results

Metabolic Stability. Figure 1 shows the metabolic stability of SMART-H in the presence and absence of NADPH and UDP-glucuronic acid. In the absence of NADPH, more than 85% of the parent SMART-H remained after 120 min, suggesting that metabolism of SMART-H was NADPH-dependent. In the presence of NADPH, SMART-H had a half-life of 17 min by phase I reaction, suggesting that SMART-H was rapidly metabolized by phase I metabolic processes. The half-life (17 min) in the presence of UDP-glucuronic acid was identical to that observed in its absence (Fig. 1). Thus, SMART-H exhibited moderate to high in vitro clearance in human liver microsomes exclusively through a phase I reaction.

Prediction of the In Vivo Clearance of SMART-H in Mouse, Rat, Dog, and Human. Table 1 summarizes in vitro half-lives (in liver microsomes), protein binding (in plasma and liver microsomes), and clearance predictions in mouse, rat, dog, and human samples. Half-lives were <5, 31, 19, and 17 min for mouse, rat, dog, and human, respectively, indicating that SMART-H exhibited interspecies variability in its metabolism. The protein-binding results indicated that SMART-H is highly protein bound (>90% bound) in plasma and liver microsomes of all four species. With high protein binding, SMART-H was predicted to have low hepatic clearances and extraction rates (≤0.3) in rat, dog, and human. Mouse was an exception. SMART-H was extremely unstable in mouse liver microsomes. Therefore, a high clearance and extraction rate were predicted in this species. Encouragingly, in vitro protein binding and metabolic stability further suggested that humans will have a low hepatic extraction ratio and low clearance.

Pharmacokinetic Studies of SMART-H. A single dose intravenous bolus of SMART-H was administered to ICR mice, Sprague-

TABLE 1

Prediction of in vivo hepatic clearance of SMART-H in mouse, rat, dog, and human from in vitro data

Hepatic blood flow values were referenced from Davies and Morris (1993).

	Mouse	Rat	Dog	Human
Hepatic blood flow (ml/min/kg)	90	55	30	21
$f_{u,p}$ in plasma (%)	0.64	0.55	0.50	0.22
$f_{u,m}$ in liver microsomes (%)	6.14	6.20	2.28	3.55
$t_{1/2}$, in liver microsomes (min)	≪5	31	19	17
Scaling factor	N.A.	2400	1815	1980
Scaling factor (mg of protein/g liver · g of liver/kg b.wt.)	N.A.	(54 · 45)	(55 · 33)	(77 · 25.7)
$Cl_{i,\ in\ vitro}$	N.A.	0.022	0.036	0.041
$Cl_{i,h}$	N.A.	53.65	66.20	80.71
Cl_h (ml/min/kg)	N.A.	4.38	9.78	4.04
Extraction rate, prediction	High	0.1	0.3	0.2

N.A., not available.

Downloaded from dmd.aspetjournals.org at ASPET Journals on March 18, 2015

Dawley rats, and a beagle dog to characterize the pharmacokinetics in these species (Fig. 2). Their PK parameters are summarized in Table 2. In vivo clearances were 130, 5.3, and 2.7 ml/min/kg for mouse, rat, and dog, respectively (Table 2), indicating a high hepatic extraction ratio (>0.7) for mouse and low extraction ratios (<0.3) for rat and dog. These data were consistent with our predictions based on in vitro data, suggesting that prediction of in vivo clearance based on in vitro protein binding and metabolic stability was reliable. In mouse, SMART-H clearance was higher than 90 ml/min/kg (the hepatic blood flow rate in mice), suggesting that in addition to hepatic removal, other degradation routes may be involved in the elimination of SMART-H in this species. Although SMART-H exhibited high protein binding in mouse, it did not compensate for instability in mouse liver microsomes. These data suggest that metabolic stability of SMART-H was critical for hepatic clearance. Intermediate volumes of distribution of 4.9 and 11 l/kg were obtained for mouse and rat. However, a smaller value of 0.4 l/kg was obtained in the dog, suggesting that SMART-H also exhibited species difference in volume of distribution. SMART-H exhibited long half-lives (more than 24 h) in both rat and dog, whereas a short half-life was obtained in mouse because of its high clearance.

Identification of Metabolites in Human Liver Microsomes. In vitro metabolite identification studies were performed using human liver microsomes to identify metabolically labile sites (i.e., soft spots) in the SMART-H pharmacophore. LC-MS/MS was used for metabolite identification based on mass shifts compared with the molecular ion $[M + H]^+$ and retention time shifts to the parent SMART-H. To identify the potential metabolites, the product ion scan for each peak of interest was examined to obtain structural information. Four major metabolites of SMART-H were identified in human liver microsomes. Figure 3A shows the multiple reaction monitoring chromatography of SMART-H with its four metabolites (M1–M4) after the 2-h incubation. Because of the high polarity exhibited by the hydroxyl groups, all of the metabolites had a shorter retention time than SMART-H. Two metabolites, M2 and M3, were present as isomers and were separated based on the gradient chromatographic condition. The product ion spectrum of SMART-H (Fig. 3B) had an abundant product ion *m/z* 188 (loss of trimethoxybenzene). The major and most abundant metabolite, M1 (*m/z* 358, mass shifts + 2 Da, ketone reduction) (Fig. 3C), resulted in the fragment ion *m/z* 340 (loss of H_2O). This metabolite was synthesized, and the retention time and product ion spectrum were confirmed (data not shown). This metabolite demonstrated altered fragment ion spectra compared with SMART-H and thus could not be detected by either precursor ion or neutral loss scans. M2 (*m/z* 342, mass shifts − 14 Da, demethylation) (Fig. 3D) was the second most abundant metabolite of SMART-H in human liver microsomes with the same fragment ion pathway and product ion *m/z* as the parent SMART-H. M2 was present as both the 3- and 4-demethylated metabolites of SMART-H, which were separated by our chromatographic conditions. However, we were unable to distinguish which of the methoxy groups were demethylated. M3 (*m/z* 344, mass shift − 12 Da, ketone reduction and demethylation) (Fig. 3E) demonstrated a fragmentation pattern similar to M1 and was apparently formed after M1. The major fragment ion of M3 was *m/z* 326 (loss of H_2O). M3 exhibited the shortest retention time because of the presence of two hydroxyl groups. M4 (*m/z* 374, mass shift + 16 Da, hydroxylation) (Fig. 3F) was an oxidized metabolite, having a hydroxyl group on the B-ring and fragmentation pattern similar to that of M1. The demethylated metabolite (M2) was the only one to be detected by the precursor ion scan (precursor of *m/z* 188). On the contrary, other metabolites exhibited different fragmentation patterns and could be detected by neither precursor ion (precursor of 188) nor by natural loss scan (loss of *m/z* 170) based on the fragmentation pattern of SMART-H fragmentation pattern. The metabolite pathway of SMART-H is summarized in Fig. 4.

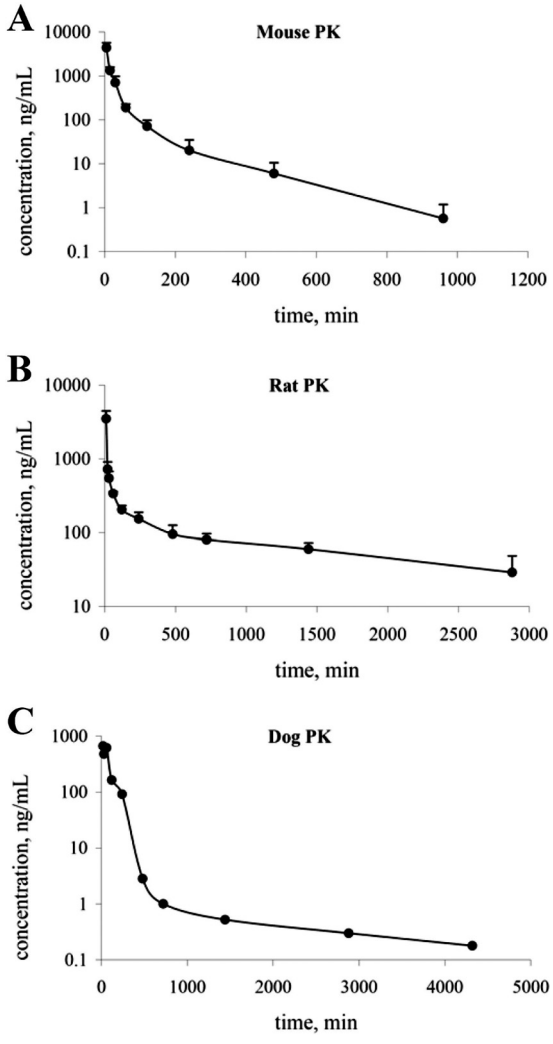

FIG. 2. Pharmacokinetic studies of SMART-H in mouse (A), rat (B), and dog (C). A single intravenous bolus administration was given with 15, 2.5, and 0.25 mg/kg for mouse ($n = 3$), rat ($n = 4$), and dog ($n = 1$), respectively. Bars, S.D.

TABLE 2

Pharmacokinetic parameters of SMART-H in mouse, rat, and dog

The half-life is presented as harmonic mean ± pseudo-S.D. in rat.

	Mouse	Rat	Dog
n	3	4	1
Dose (mg/kg)	15	2.5	0.25
Volume of distribution, V_{ss} (l/kg)	4.9	11 ± 4	0.4
AUC (h · mg/ml)	1.9	5.8 ± 1.1	1.6
K_e (min^{-1})	0.0049	0.00032 ± 0.000045	0.0004
Half-life, $t_{1/2}$ (min)	140	2143 ± 292	1866
Clearance (ml/min/kg)	130	5.3 ± 0.9	2.7
Hepatic blood flow (ml/min/kg)	90	55	30
Extraction rate	>1	0.1	0.1

AUC, area under the concentration-time curve.

Species-Specific Metabolism of SMART-H. We determined the metabolite kinetics of SMART-H (0.5 μM) in the presence of liver microsomes from mouse, rat, dog, and human. The parent, SMART-H, and the four metabolites identified in human liver microsomes were simultaneously monitored in each sample (Fig. 5). The half-lives of SMART-H in microsomes from different species

Downloaded from dmd.aspetjournals.org at ASPET Journals on March 18, 2015

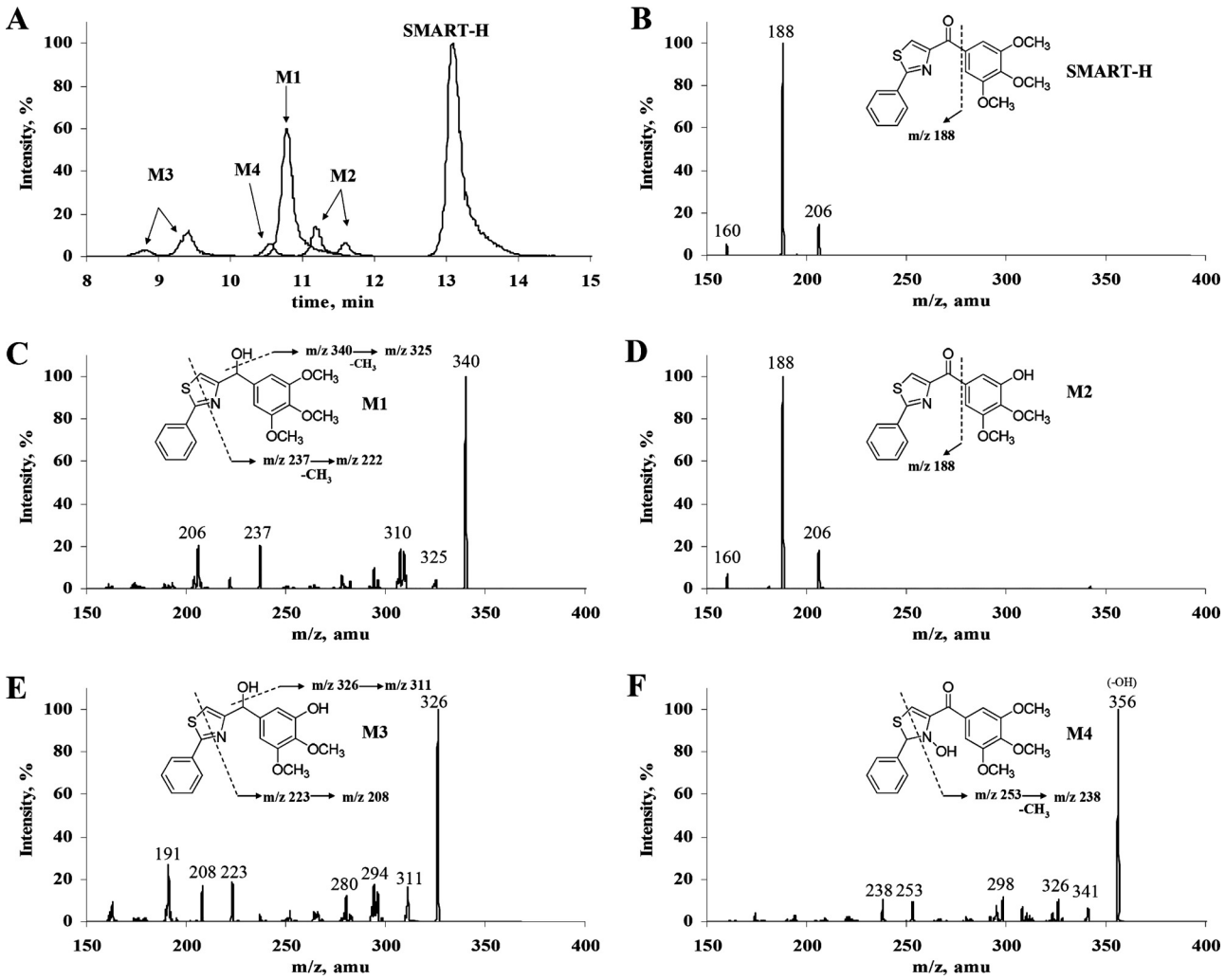

FIG. 3. Metabolite identification. SMART-H (50 μM) was incubated with 1 mg/ml human liver microsomes for 2 h. A, chromatography. B, MS/MS spectrum of parent SMART-H. Four major MS/MS spectra were identified in M1 (C), M2 (D), M3 (E), and M4 (F).

varied over a broad range from <5 to 30 min (Fig. 5; Table 1). We found that the metabolite arising from ketone reduction (M1) was dominant only in human liver microsomes. We then increased the SMART-H concentration from 0.5 to 50 μM and incubated with 1 mg/ml human and rat liver microsomes to saturate the enzymes and maximize the metabolite signals (Fig. 6). The demethylated metabolite, M2, was found in microsomal incubation using both rat and human liver microsomes. A significant difference in M1 and M3 levels was observed between the two species. In rat liver microsomes (Fig. 6B), the primary metabolite was the demethylated metabolite (M2). M1 could be found in rat liver microsomes only when a higher concentration of SMART-H was used. However, the amount of M1 in rat liver microsomes was much less than that in human liver microsomes (Fig. 6). In addition, the relative amount of the demethylated metabolite (M2) in rat liver microsomes was greater than that in the human liver microsomes. These studies confirmed that M1 was a dominant metabolite only in human liver microsomes.

Blockage of Soft Spots of SMART-H to Increase the Metabolic Stability in Human Liver Microsomes. The two major metabolites in human liver microsomes, M1 (ketone reduction) and M2 (demethylation), identified the carbonyl and methoxy groups as the most labile sites (i.e., soft spots) to metabolic conversion. We thus designed the next generation of SMART compounds to include substitutions aimed to improve the metabolic stability of these soft spots. Three compounds (SMART-329, -173A, and -176A) with modified or direct linkage between the trimethoxyphenyl ring and thiazole ring were made and tested, and a single compound (SMART-213) with a pentafluoro phenyl ring was made to replace the trimethoxy substituents (Fig. 7). The inclusion of a pentafluoro phenyl ring (SMART-213) failed to increase metabolic stability in human liver microsomes (Fig. 8), suggesting that demethylation may not be critical for metabolic stability or that SMART-213 was susceptible to other new metabolic pathways. We also examined the metabolic stability of analogs containing electron-withdrawing substituents such as 4-fluorophenyl or 3,4,5-trifluorophenyl to replace the trimethoxyphenyl ring. All of these derivatives failed to increase the metabolic stability (data not shown). A dramatic increase in the metabolic stability was observed with compound SMART-176A which contains C═N–NH_2 instead of C═O found in SMART-H. This compound exhibited 3-fold longer stability than that of our lead compound, SMART-H, in human liver microsomes. SMART-173A and SMART-329 also demonstrated an increase in metabolic stability by 2-fold. These data indicate that the enhanced metabolic stability observed in human liver microsomes correlated with the modification of the labile ketone site of SMART-H.

Table 3 shows IC_{50} values of SMART-213, -173A, -176A, and -329 for antiproliferative effects on four prostate cancer cell lines,

Downloaded from dmd.aspetjournals.org at ASPET Journals on March 18, 2015

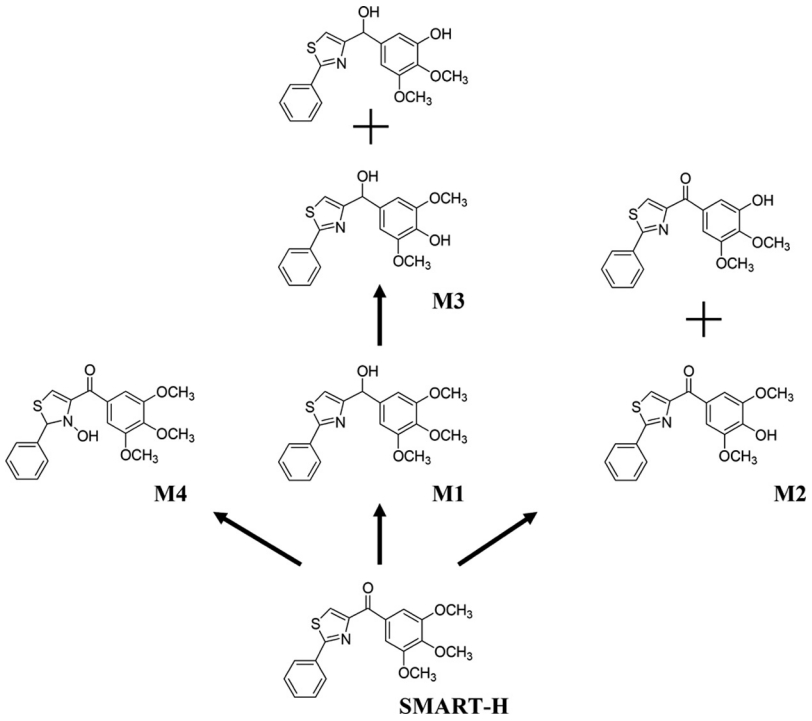

FIG. 4. Metabolite profile of SMART-H in human liver microsome.

LNCaP, PC-3, DU 145, and PPC-1. SMART-173A retained potent activity with an average IC_{50} value of 143 nM. SMART-176A had less potent ability (IC_{50} value of 1250 nM) to inhibit cell proliferation. With the removal of the labile functional group (C═O), SMART-329 demonstrated increased metabolic stability; however, it lost the ability to inhibit cell growth (IC_{50} value was >10,000 nM). SMART-213 failed to either inhibit cell growth or improve metabolic stability. These results indicate that blocking ketone reduction increased metabolic stability in human liver microsomes but that in vitro anticancer activity could only be partially retained by substituting with the oxime (SMART-173A).

Discussion

In vitro microsomal stability assays represent a high-throughput method to predict in vivo hepatic clearance. Here, we used mice, rats, and dog to study the in vitro-in vivo relationship of SMART-H metabolism. The in vitro metabolic stability of SMART-H was extremely poor in mouse liver microsomes, resulting in the high clearance value obtained during in vivo pharmacokinetic studies in mice. The in vivo total clearance in rats was 5.3 ml/min/kg, which is close to our prediction based on in vitro microsomal stability studies. The in vivo total clearance in dog was 2.7 ml/min/kg, which was somewhat smaller than our prediction. In mouse, rat, and dog pharmacokinetic studies, the distributional kinetics, not the long terminal phase, seem to define most of the area under the concentration-time curve (Fig. 2). The in vitro value for dogs may have been overestimated as a result of errors in the scaling factor or determination of fraction unbound in plasma and liver microsomes, whereas the predicted clearance value for mice slightly underestimated the in vivo clearance apparently as a result of extrahepatic drug clearance. The in vivo clearance values for

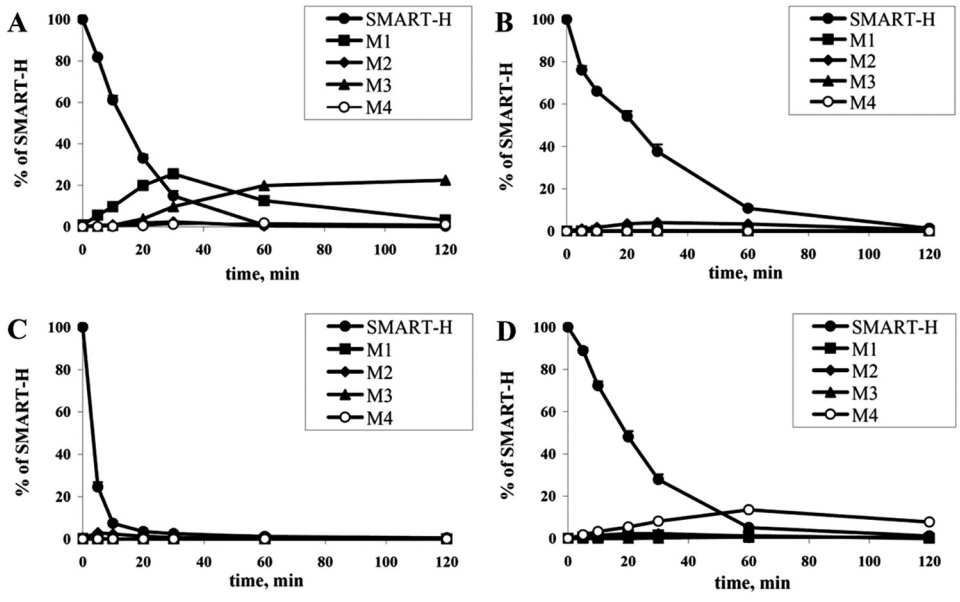

FIG. 5. Metabolite profile in species. Substrate (0.5 μM) was incubated with 1 mg/ml microsomal protein of human (A), rat (B), mice (C), and dog (D). Four metabolites with the parent were measured by LC-MS/MS (n = 3). Bars, SD.

Downloaded from dmd.aspetjournals.org at ASPET Journals on March 18, 2015

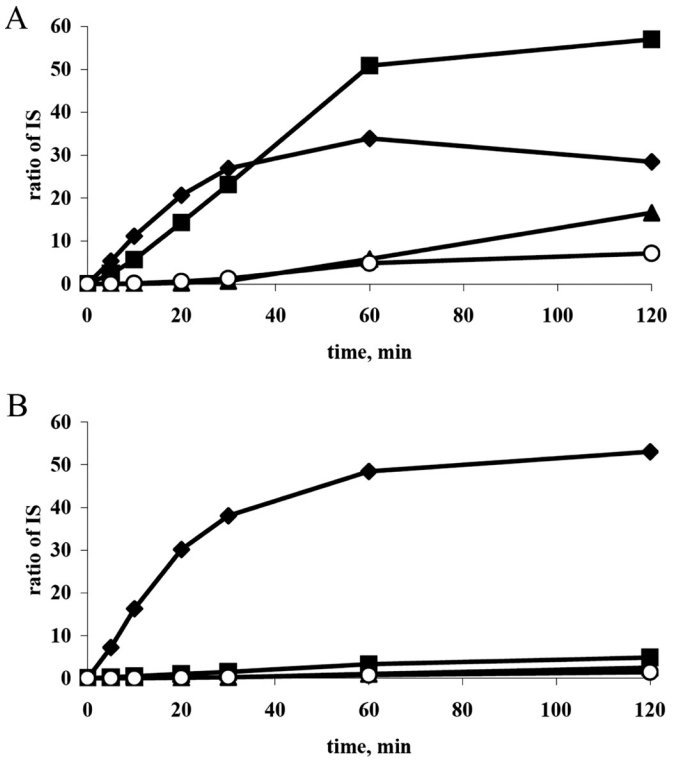

FIG. 6. Kinetics of four metabolites of SMART-H in human liver microsome (A) and rat liver microsome (B). SMART-H (50 μM) was incubated with 1 mg/ml microsomal proteins. ■, M1; ♦, M2; ▲, M3; ○, M4.

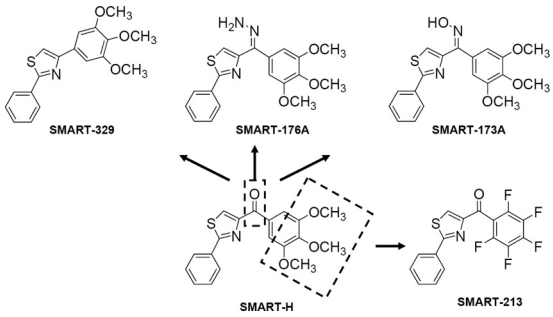

FIG. 7. Blockage of soft spots.

rat and dog were lower than expected on the basis of their in vitro metabolic stability without considering protein binding. These low clearance data are reasonable when the high protein binding of SMART-H is considered, demonstrating that high protein binding of SMART-H reduced its in vivo clearance. However, high protein binding did not preclude high clearance when the metabolic stability was poor, as seen in mice.

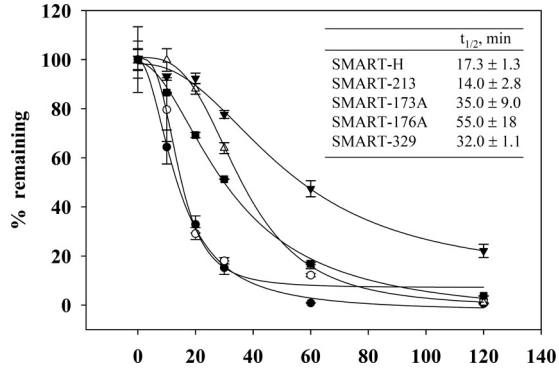

FIG. 8. Metabolic stability of SMART-H (●), SMART-213 (○), SMART-173A (□), SMART-176A (▼), and SMART-329 (■) in human liver microsome. Bar, S.D.

TABLE 3

Antiproliferation of SMART compounds on prostate cancer cell lines

$n = 3$.

	IC_{50}			
	LNCaP	PC-3	DU 145	PPC-1
	nM			
SMART-H	33	26	73	41
SMART-213	>10,000	>10,000	>10,000	>10,000
SMART-329	>10,000	>10,000	>10,000	>10,000
SMART-173A	189	120	102	160
SMART-176A	1800	1120	1210	872

Although SMART-H demonstrated reasonable metabolic stability during incubation with rat, dog, and human liver microsomes, notable differences in the relative quantities and identity of the metabolites formed in different species were observed (Fig. 6). Because such differences would complicate future toxicological assessment and interspecies comparisons, we sought to define these differences and evaluate structurally optimized SMART compounds with improved metabolic stability and potent anticancer activity.

In metabolite identification studies in rat liver microsomes, the *O*-demethylated metabolite (M2) was the major metabolite. M2 was found in a time-dependent manner when 50 μM substrate was used. The level of the *O*-demethylated metabolite was much greater than that of the ketone-reduced (M1) metabolite. This phenomenon was confirmed by in vivo experiments. In rat PK (dose of 2.5 mg/kg i.v.) studies, we compared the metabolite levels in plasma samples (supplemental data). Only the *O*-demethylated (M2) and ketone-reduced metabolites (M1) could be detected in rat plasma. The M2 metabolite exhibited approximately 10-fold higher exposure than M1 metabolite in rat plasma. These data further corroborate the conclusion that in vitro metabolic stability is a good predictor of in vivo pharmacokinetics.

Our ultimate goal is to develop an anticancer drug for use in humans with appropriate PK properties. In this study, SMART-H exhibited a half-life of 17 min in human liver microsomes, suggesting that additional measures could be taken to improve its metabolic stability. The metabolic kinetic profiles in rat and human suggested that ketone reduction was an important metabolic pathway in humans but not in rats, because of the apparent presence of M1 in humans (Fig. 6). We speculated that modifying the ketone functional group would improve the metabolic stability in human liver microsomes. Blocking or removing labile sites is a common strategy to increase metabolic stability. In this study, we synthesized three analogs (SMART-173A, -176A, and -329) to prevent the ketone reduction reaction. The half-lives were longer (35, 55, and 32 min, respectively) in human liver microsomes, indicating that the ketone site is a critical soft spot for improving metabolic stability in humans. The in vitro metabolic stability of SMART-176A, a hydrazine derivative, was not tested using conditions suitable for acetylation (perhaps resulting in an overestimate of its stability) but failed to retain anticancer activity. SMART-173A retained its potency, with an average IC_{50} value of 143 nM in four prostate cancer cell lines.

In summary, the studies presented here predict that SMART-H will exhibit low clearance in humans based on in vitro data. However, our studies also suggest that the metabolic stability of SMART-H and its analogs can be further optimized to obtain prolonged half-life and increased exposure in humans. Metabolism studies demonstrate that

Downloaded from dmd.aspetjournals.org at ASPET Journals on March 18, 2015

SMART-H was rapidly metabolized under phase I reactions in human liver microsomes. Ketone reduction and *O*-demethylation reactions were the primary metabolic pathways for SMART-H. The metabolic stability (half-life) was successfully improved two to three times in vitro by blocking the ketone group. Although SMART-173A, the oxime derivative with C═N–OH instead of C═O of SMART-H, demonstrated greater metabolic stability, the in vitro potency was compromised as evidenced by a nearly equal increase in IC_{50} in prostate cancer cell lines. Studies to identify additional analogs with improved metabolic stability that retain high potency are ongoing in our laboratory.

Acknowledgments. We thank Terrence A. Costello, Katie N. Kail, and Stacey L. Barnett for providing technical support for animal studies at GTx Inc.

References

Baarnhielm C, Dahlback H, and Skanberg I (1986) In vivo pharmacokinetics of felodipine predicted from in vitro studies in rat, dog and man. *Acta Pharmacol Toxicol (Copenh)* **59:**113–122.

Carlson RO (2008) New tubulin targeting agents currently in clinical development. *Expert Opin Investig Drugs* **17:**707–722.

Chiba M, Ishii Y, and Sugiyama Y (2009) Prediction of hepatic clearance in human from in vitro data for successful drug development. *AAPS J* **11:**262–276.

Davies B and Morris T (1993) Physiological parameters in laboratory animals and humans. *Pharm Res* **10:**1093–1095.

Huang M and Ho PC (2009) Identification of metabolites of meisoindigo in rat, pig and human liver microsomes by UFLC-MS/MS. *Biochem Pharmacol* **77:**1418–1428.

Lu Y, Li CM, Wang Z, Ross CR 2nd, Chen J, Dalton JT, Li W, and Miller DD (2009) Discovery of 4-substituted methoxybenzoyl-aryl-thiazole as novel anticancer agents: synthesis, biological evaluation, and structure-activity relationships. *J Med Chem* **52:**1701–1711.

Pelkonen O, Turpeinen M, Uusitalo J, Rautio A, and Raunio H (2005) Prediction of drug metabolism and interactions on the basis of in vitro investigations. *Basic Clin Pharmacol Toxicol* **96:**167–175.

Perez EA (2009) Microtubule inhibitors: differentiating tubulin-inhibiting agents based on mechanisms of action, clinical activity, and resistance. *Mol Cancer Ther* **8:**2086–2095.

Smith R, Jones RD, Ballard PG, and Griffiths HH (2008) Determination of microsome and hepatocyte scaling factors for in vitro/in vivo extrapolation in the rat and dog. *Xenobiotica* **38:**1386–1398.

Sun L, Vasilevich NI, Fuselier JA, and Coy DH (2004) Abilities of 3,4-diarylfuran-2-one analogs of combretastatin A-4 to inhibit both proliferation of tumor cell lines and growth of relevant tumors in nude mice. *Anticancer Res* **24:**179–186.

Zhang H, Zhang D, Li W, Yao M, D'Arienzo C, Li YX, Ewing WR, Gu Z, Zhu Y, Murugesan N, et al. (2007) Reduction of site-specific CYP3A-mediated metabolism for dual angiotensin and endothelin receptor antagonists in various in vitro systems and in cynomolgus monkeys. *Drug Metab Dispos* **35:**795–805.

Zhao Y, Fang WS, and Pors K (2009) Microtubule stabilising agents for cancer chemotherapy. *Expert Opin Ther Pat* **19:**607–622.

Address correspondence to: Dr. James T. Dalton, GTx Inc., 3 N. Dunlap St., Memphis TN 38163. E-mail: jdalton@gtxinc.com

Downloaded from dmd.aspetjournals.org at ASPET Journals on March 18, 2015